MEAN SQUARE ANALYSIS OF A FAST FILTERED-X AFFINE PROJECTION ALGORITHM

Miguel Ferrer, Alberto González, María de Diego and Gema Piñero[*]

Audio and Communications Signal Processing Group (GTAC)
Institute of Telecommunications and Multimedia Applications (iTEAM)
Universidad Politécnica de Valencia
http://www.gtac.upv.es
mferrer@dcom.upv.es

ABSTRACT

This paper provides an analysis of the steady-state behavior of the filtered-x affine projection algorithm (FXAP). This efficient affine projection (AP) algorithm for active noise control (ANC) applications is based on the filtered-x scheme, unlike most AP algorithms based on the more computationally demanding modified filtered-x scheme. This study depends on energy conservation arguments and does not require an specific signal distribution. The theoretical expressions derived for the mean square error (MSE) allowed to accurately predict the steady-state performance of the FXAP for meaningful practical cases. Simulation results of a single-channel ANC system validate the analysis and the theoretical expressions derived.

Index Terms— Adaptive control, Acoustic noise, Transversal filters, Steady state stability.

1. INTRODUCTION

In the ANC field, affine projection (AP) algorithms have demonstrated to be very helpful to outperform the convergence properties of the conventional adaptive filters usually applied [1, 2] with a moderate computational effort. Most of the AP algorithms proposed, including their computationally efficient versions, are based on the modified filtered-x scheme. However, a fast AP algorithm based on the filtered-x scheme (FXAP), was recently proposed in [3] for multichannel ANC systems, see Fig. 1.

Despite the existing interest in this kind of algorithms, very few works have been published in reference to their convergence properties. Among the different approaches, the analysis developed in [4] for AP algorithms is based on energy conservation arguments and does not depend on the input signal distribution. This approach was applied in the context of ANC using the AP algorithm with the modified filtered-x scheme [5]. In the present paper, the methodology presented in [4] is applied to the FXAP algorithm based on the filtered-x scheme to study its steady-state properties.

2. FILTERED-X AFFINE PROJECTION ALGORITHM

The filtered-x affine projection algorithm (FXAP) described in [3] is an efficient version of the AP algorithm [6] based on the filtered-x scheme. The update equation of the AP adaptive filter coefficients in the single-channel case reads as:

$$\mathbf{w}_L[n] = \mathbf{w}_L[n-1] - \mu \mathbf{V}^T[n](\mathbf{V}[n]\mathbf{V}^T[n] + \delta I)^{-1}\mathbf{e}_N[n], \quad (1)$$

where δ is a regularization parameter [7], μ is a convergence parameter [2] and $\mathbf{e}_N[n]$ is called the error vector. Moreover, $\mathbf{w}_L[n]$ is a vector comprised of the L adaptive filter coefficients at the nth time instant. Matrix $\mathbf{V}[n]$ of dimensions $N \times L$ contains the filtered reference signal values as follows:

$$\mathbf{V}^T[n] = [\mathbf{v}_L[n], \mathbf{v}_L[n-1], ..., \mathbf{v}_L[n-N+1]], \quad (2)$$

where $\mathbf{v}_L[n]$ is a vector with the more recent L samples of the reference signal $x[n]$ filtered through a version $\hat{S}$ of the secondary path, and N is called the affine projection order [6]. The objective is to estimate the L-dimensional optimal coefficient vector $\mathbf{w}_L^o$, such that the desired signal vector was given by $\mathbf{d}_N[n] = -\mathbf{V}[n]\mathbf{w}_L^o$. However, this result is not achieved in practice [4] and it is more meaningful to use,

$$\mathbf{d}_N[n] = -\mathbf{V}[n]\mathbf{w}_L^o + \mathbf{r}_N[n] \quad (3)$$

being $\mathbf{r}_N[n]$ a $N \times 1$ Gaussian noise vector of zero mean and σ_r^2 variance, uncorrelated with data signal.

The error vector $\mathbf{e}_N[n]$, built by past samples of error signal $e[n]$, can be expressed as:

$$\begin{aligned}\mathbf{e}_N[n] &= \mathbf{d}_N[n] + \begin{pmatrix} \mathbf{v}_L^T[n]\mathbf{w}_L[n-1] \\ \mathbf{v}_L^T[n-1]\mathbf{w}_L[n-2] \\ \vdots \\ \mathbf{v}_L^T[n-N+1]\mathbf{w}_L[n-N] \end{pmatrix} \\ &= \mathbf{e}_N^{a'}[n] + \mathbf{r}_N[n].\end{aligned} \quad (4)$$

Likewise, we have defined the particular *a priori* error vector $\mathbf{e}_N^{a'}[n]^T$ by:

$$\begin{aligned}\mathbf{e}_N^{a'}[n]^T &= \begin{pmatrix} e_v^a[n] \\ e_v^a[n-1] \\ \vdots \\ e_v^a[n-N+1] \end{pmatrix} \\ &= \begin{pmatrix} \mathbf{v}_L^T[n](\mathbf{w}_L[n-1] - \mathbf{w}_L^o) \\ \mathbf{v}_L^T[n-1](\mathbf{w}_L[n-2] - \mathbf{w}_L^o) \\ \vdots \\ \mathbf{v}_L^T[n-N+1](\mathbf{w}_L[n-N] - \mathbf{w}_L^o) \end{pmatrix}.\end{aligned} \quad (5)$$

[*] This work was partially funded by CICYT grant TEC2006-13883-C04-01.

3. STEADY-STATE ANALYSIS

In the steady-state analysis we are interested in the limit for $n \rightarrow \infty$ of the mean square error, MSE. That is,

$$\text{MSE} = \lim_{n\rightarrow\infty} E\{|e[n]|^2\} \tag{6}$$

or equivalently, in the excess mean square error (EMSE)

$$\text{EMSE} = \lim_{n\rightarrow\infty} E\{|e_v^a[n]|^2\} \tag{7}$$

that are related by:

$$\text{MSE} = \text{EMSE} + \sigma_r^2, \tag{8}$$

being σ_r^2 the noise variance.

Following the approach shown in [4], a recursion for $\|w[n]\|^2$ based on the energy conservation relation can be derived, where $||\cdot||$ denotes the Euclidean norm. Firstly equation (1) can be rewritten in terms of the coefficient error vector, $\widetilde{\mathbf{w}}_L[n] = \mathbf{w}_L[n] - \mathbf{w}_L^o$, and then it holds,

$$\widetilde{\mathbf{w}}_L[n] = \widetilde{\mathbf{w}}_L[n-1] - \mu\mathbf{V}^T[n](\mathbf{V}[n]\mathbf{V}^T[n] + \delta I)^{-1}\mathbf{e}_N[n]. \tag{9}$$

Let be $\mathbf{e}_{vN}^a[n]$ and $\mathbf{e}_{vN}^p[n]$ the *a priori* and *a posteriori* error vectors, respectively:

$$\mathbf{e}_{vN}^a[n] = \mathbf{V}[n]\widetilde{\mathbf{w}}_L[n-1], \quad \mathbf{e}_{vN}^p[n] = \mathbf{V}[n]\widetilde{\mathbf{w}}_L[n]. \tag{10}$$

Then, suitably manipulating and taking energies at both sides of (9), the energy conservation relation is obtained,

$$\begin{aligned}&\|\widetilde{\mathbf{w}}_L[n]\|^2 + (\mathbf{e}_{vN}^a[n])^T(\mathbf{V}[n]\mathbf{V}^T[n])^{-1}\mathbf{e}_{vN}^a[n] = \\ &\quad \|\widetilde{\mathbf{w}}_L[n-1]\|^2 + (\mathbf{e}_{vN}^p[n])^T(\mathbf{V}[n]\mathbf{V}^T[n])^{-1}\mathbf{e}_{vN}^p[n].\end{aligned} \tag{11}$$

Note that the energies of the coefficient error vectors at different iterations are related to the weighted energies of the *a priori* and *a posteriori* error vectors, just as the relation provided in [4]. Applying the expectation operator $E\{\cdot\}$ at both sides of (11) and the steady-state conditions ($E\{\|\widetilde{\mathbf{w}}_L[n]\|^2\} = E\{\|\widetilde{\mathbf{w}}_L[n-1]\|^2\}$ as $n \rightarrow \infty$), it becomes

$$\begin{aligned}&\mu E\{(\mathbf{e}_N^{a'}[n])^T\mathbf{\Psi}_v[n]\mathbf{e}_N^{a'}[n]\} + \mu E\{\mathbf{r}_N^T[n]\mathbf{\Psi}_v[n]\mathbf{r}_N[n]\} = \\ &\quad = 2E\{(\mathbf{e}_N^{a'}[n])^T\mathbf{\Phi}_v[n]\mathbf{e}_{vN}^a[n]\}\end{aligned} \tag{12}$$

where the following matrices are defined

$$\begin{aligned}\mathbf{\Phi}_v[n] &= (\mathbf{V}[n]\mathbf{V}^T[n] + \delta I)^{-1} \quad \text{and} \\ \mathbf{\Psi}_v[n] &= \mathbf{\Phi}_v[n](\mathbf{V}[n]\mathbf{V}^T[n])\mathbf{\Phi}_v[n].\end{aligned} \tag{13}$$

Assuming statistical independence between data related matrices and the other involved vectors, and also the equality for two column vectors of length N, $\mathbf{a}^T\mathbf{b} = Tr(\mathbf{a}\mathbf{b}^T)$, it yields

$$\begin{aligned}&\mu Tr(E\{\mathbf{e}_N^{a'}[n](\mathbf{e}_N^{a'}[n])^T\}E\{\mathbf{\Psi}_v[n]\}) \\ &+\mu Tr(E\{\mathbf{r}_N[n](\mathbf{r}_N[n])^T\}E\{\mathbf{\Psi}_v[n]\}) \\ &= 2Tr(E\{\mathbf{e}_N^{a'}[n](\mathbf{e}_{vN}^a[n])^T\}E\{\mathbf{\Phi}_v[n]\}).\end{aligned} \tag{14}$$

Next, some simplifications and assumptions are applied to the different terms in (14). When $n \rightarrow \infty$ and neglecting off-diagonal terms of the $E\{\mathbf{e}_N^{a'}[n](\mathbf{e}_N^{a'}[n])^T\}$ matrix, the first term on the left hand side of (14) reduces to

$$\begin{aligned}&\mu Tr(E\{\mathbf{e}_N^{a'}[n](\mathbf{e}_N^{a'}[n])^T\}E\{\mathbf{\Psi}_v[n]\}) \\ &\quad = \mu E \mid e_v^a[n] \mid^2 Tr(E\{\mathbf{\Psi}_v[n]\}),\end{aligned} \tag{15}$$

being $e_v^a[n]$ the top element of the particular *a priori* error vector $\mathbf{e}_N^{a'}[n]$.

The second term, related with the noise vector, simplifies to

$$\begin{aligned}&\mu Tr(E\{\mathbf{r}_N[n](\mathbf{r}_N[n])^T\}E\{\mathbf{\Psi}_v[n]\}) \\ &\quad = \mu\sigma_r^2 Tr(E\{\mathbf{\Psi}_v[n]\}).\end{aligned} \tag{16}$$

On the other hand, the term on the right hand side of (14) can be simplified by means of similar considerations. Using (4) and (10) when δ is small, we get that

$$\mathbf{e}_{vN}^p[n] = \mathbf{e}_{vN}^a[n] - \mu\mathbf{e}_N^{a'}[n] - \mu\mathbf{r}_N[n]. \tag{17}$$

Then, the following relations can be derived,

$$\begin{aligned}&E\{\mathbf{v}_L^T[n]\widetilde{\mathbf{w}}_L[n-1]\mathbf{v}_L^T[n]\widetilde{\mathbf{w}}_L[n-1]\} = E\{|e_v^a[n]|^2\}, \\ &E\{\mathbf{v}_L^T[n-1]\widetilde{\mathbf{w}}_L[n-2]\mathbf{v}_L^T[n-1]\widetilde{\mathbf{w}}_L[n-1]\} \\ &\qquad = (1-\mu)E\{|e_v^a[n-1]|^2\}, \\ &\quad \vdots \\ &E\{\mathbf{v}_L^T[n-N+1]\widetilde{\mathbf{w}}_L[n-N]\mathbf{v}_L^T[n-N+1]\widetilde{\mathbf{w}}_L[n-1]\} \\ &\qquad = [1-(N-1)\mu]E\{\mid e_v^a[n-N+1] \mid^2\},\end{aligned} \tag{18}$$

and since in steady-state $\{|e_v^a[n]|^2\} = E\{|e_v^a[n-1]|^2\} = \ldots = E\{|e_v^a[n-N+1]|^2\}$, it leads to

$$E\{\mathbf{e}_N^{a'}[n](\mathbf{e}_{vN}^a[n])^T\} \approx E\{\mid e_v^a[n] \mid^2\}D_1, \tag{19}$$

where the diagonal matrix D_1 is given by:

$$D_1 = \begin{pmatrix} 1 & & & & \\ & (1-\mu) & & & \\ & & (1-2\mu) & & \\ & & & \ddots & \\ & & & & (1-(N-1)\mu) \end{pmatrix}. \tag{20}$$

Finally, equation (14) becomes

$$\begin{aligned}&\mu E\{\mid e_v^a[n] \mid^2\}Tr(E\{\mathbf{\Psi}_v[n]\}) + \mu\sigma_r^2 Tr(E\{\mathbf{\Psi}_v[n]\}) \\ &\quad = 2E\{\mid e_v^a[n] \mid^2\}Tr(E\{D_1\mathbf{\Phi}_v[n]\})\end{aligned} \tag{21}$$

and the EMSE of the corresponding filter is given by

$$\text{EMSE} = \frac{\mu\sigma_r^2 Tr(E\{\mathbf{\Psi}_v[n]\})}{2Tr(E\{D_1\mathbf{\Phi}_v[n]\}) - \mu Tr(E\{\mathbf{\Psi}_v[n]\})}. \tag{22}$$

This expression can be simplified when the regularization parameter δ is small enough. Then, we get,

$$\begin{aligned}\text{EMSE} &= (\mu\sigma_r^2)\frac{Tr(E\{\mathbf{\Psi}_v[n]\})}{Tr((2D_1 - \mu\mathbf{I})E\{\mathbf{\Psi}_v[n]\})} \\ &= (\mu\sigma_r^2)\frac{Tr(E\{\mathbf{\Psi}_v[n]\})}{Tr(D_2 E\{\mathbf{\Psi}_v[n]\})},\end{aligned} \tag{23}$$

being $\mathbf{I}$ the $N \times N$ identity matrix and D_2 a diagonal matrix given by:

$$D_2 = \begin{pmatrix} (2-\mu) & & & \\ & (2-3\mu) & & \\ & & \ddots & \\ & & & (2-(2N-1)\mu) \end{pmatrix}. \tag{24}$$

Another two simplifications can be carried out depending on μ parameter values:

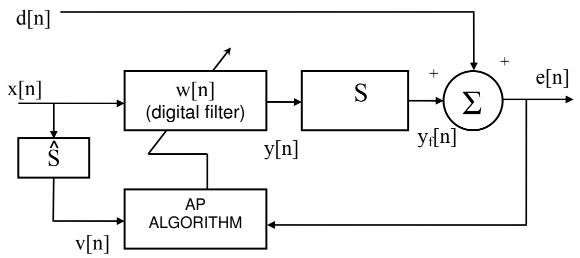

Fig. 1. Block-diagram of an ANC system using the filtered-x structure

- If μ is small, $D_2 \approx 2I$ and (23) reduces to,

$$EMSE = \frac{\mu\sigma_r^2}{2}, \tag{25}$$

- If a large μ is used, then,

$$EMSE = (\mu\sigma_r^2)\frac{Tr(E\{\mathbf{\Psi}_v[n]\})}{Tr(D_3 E\{\mathbf{\Psi}_v[n]\})}, \tag{26}$$

where

$$D_3 = \begin{pmatrix} 1 & & & & 0 \\ & -1 & & & \\ & & -3 & & \\ & & & \ddots & \\ 0 & & & & 3-2N \end{pmatrix}. \tag{27}$$

4. SIMULATION RESULTS

In this section a comparison between the theoretical predicted values and the values obtained from simulations is shown. The results are provided for a single-channel ANC system using the FXAP algorithm, see Fig. 1. The input signal is a colored Gaussian signal generated by filtering white Gaussian noise (of zero mean and unit variance) with a first order autoregressive filter of transfer function $\sqrt{1-a^2}/(1-az^{-1})$ being $a = 0{,}9$. The desired signal $d[n]$ generated by following the model in (3) with Gaussian noise of $\sigma_r^2 = 0{,}001$ and an optimal coefficient vector $\mathbf{w}_L^o$ of 16 coefficients. The secondary path was perfectly model with an 8 coefficients filter, and the adaptive filter has the same length as the unknown channel (16 coefficients).

The experimental results of MSE were obtained by averaging over 10 independent runs of $600{,}000$ samples. In addition, different step size μ values were applied for AP orders from $N = 2$ to $N = 8$. The regularization parameter δ was set to 10^{-5}. The theoretical estimation of MSE was provided by (22), (23), (25) or (26), and using (8). The range of μ values chosen is from 0.01 to 0.1 in order to guarantee stability of the adaptive algorithm, unlike the higher values allowed in [4, 5] due to the use of the modified filtered-x scheme.

Figure 2 shows the simulated MSE for different affine projections orders as a function of the step size. It is verified that the MSE worsens when μ increases. Higher values of the order N speeds up this effect for increasing μ. On the other hand, the convergence speed increases with N and μ [3].

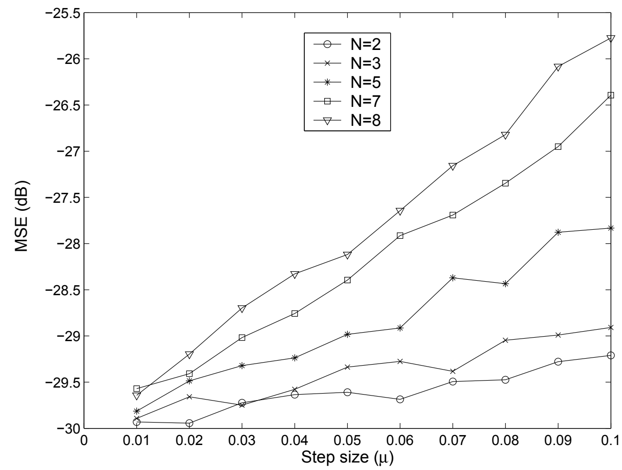

Fig. 2. *Simulated MSE in dB as a function of μ for different N orders.*

The comparison between the estimated MSE using different theoretical expressions is illustrated in Fig. 3 for $N = 6$. Also, the simulated MSE is drawn. The estimated MSE curve that better agrees with the simulation is obtained using (26), with the assumption of a large μ.

Figure 4 shows a comparison between the simulated and the estimated steady-state MSE using (26) for AP orders $N = 2$, $N = 4$ and $N = 6$. The estimated curves lie close to the simulated ones, closer for low μ values and projection orders of moderate value.

Figure 5 illustrates the evolution of the residual error of the FXAP for $N = 3$, $N = 7$ and $\mu = 0{,}02$ for the first samples. Each sample of the diagram has been estimated by an exponential windowed of 100 samples of the residual error power averaged over 10 runs, and only the transient period at the beginning of the adaptation process is shown. It can be observed the good convergence speed the FXAP exhibits, much faster as N increases [3] and very similar to the convergence performance of the AP algorithm based on the modified filtered-x structure [7].

Finally, the obtained results can be compared to the study shown in [4] and [5] and they are coherent with the evaluation results provided in those works.

5. CONCLUSIONS

In this paper, an analysis of the steady-state MSE performance of the FXAP algorithm for ANC has been presented. The methodology applied is based on energy conservation relations avoiding other more restrictive assumptions. Furthermore, the estimated steady-state behavior of the FXAP algorithm has been validated by means of simulation results provided by a single-channel ANC system. Finally, this analysis should be completed with an study of the transient performance of the FXAP.

6. REFERENCES

[1] S.C. Douglas, "The fast affine projection algorithm for active noise control," *Proceedings of the 29th Asilomar Conference*

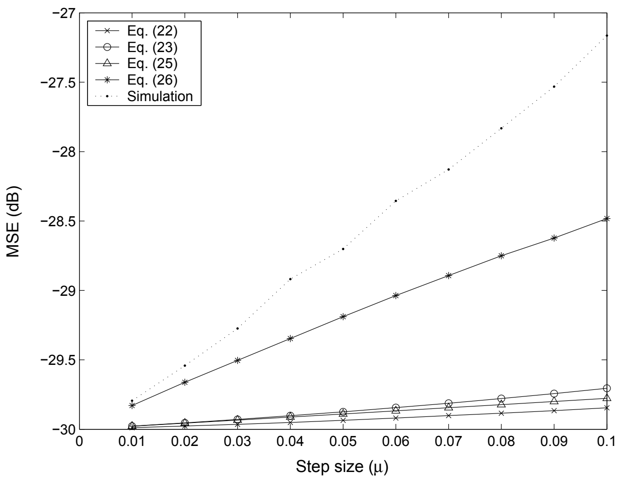

Fig. 3. *Comparison between the estimated MSE expressions and the simulated MSE, as a function of μ for $N = 6$.*

on Signals, Systems and Components, vol. 2, pp. 1245–1249, October 1995, Pacific Grove,CA.

[2] M. Bouchard, "Multichannel affine and fast affine projection algorithms for active noise control and acoustic equalization systems," *IEEE Transactions on Speech and Audio Processing*, vol. 11, no. 1, pp. 54–60, January 2003.

[3] A. Gonzlez, M. Ferrer, M. de Diego, and G. Piero, "Fast filtered-x affine projection algorithm for active noise control," *Proceedings of IEEE Workshop on Application of Signal Procesing to Audio and Acoustics WASPAA 05*, pp. 162–165, 2005.

[4] H. Shin and A. Sayed, "Mean-square performance of a family of affine projection algorihtms," *IEEE Trans. on Signal Processing*, vol. 52, no. 1, pp. 90–102, January 2004.

[5] A. Carini and G. Sicuranza, "Transient and steady-state analysis of filtered-x affine projection algorihtm," *IEEE Trans. on Signal Process.*, vol. 54, no. 2, 2006.

[6] S. Haykin, *Adaptive Filter Theory*, Prentice-Hall, Ed., Upper Saddle River, NJ, Fourth edition, 2002.

[7] A. Gonzlez, M. Ferrer, M. de Diego, and G. Piero, "Fast filtered-x affine projection algorithm with efficient computation of coefficient update," *Proceedings of IEEE Int. Conf. Acoust. Speech and Signal Processing ICASSP 2006*, pp. 285–288, 2006.

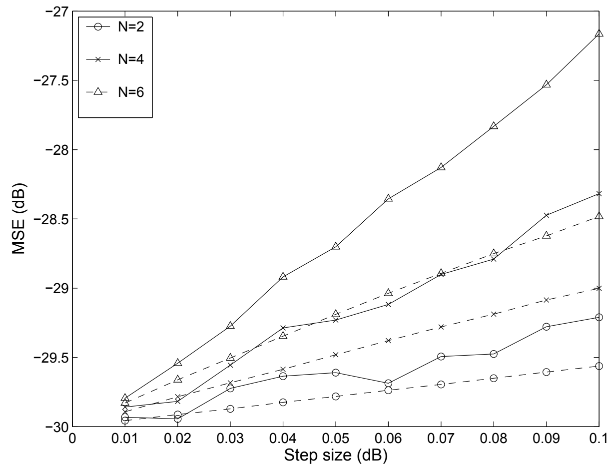

Fig. 4. *Comparison between the estimated MSE by (26) (dashed line) and the simulated MSE (solid line), as a function of μ for $N = 2$, 4 and 6.*

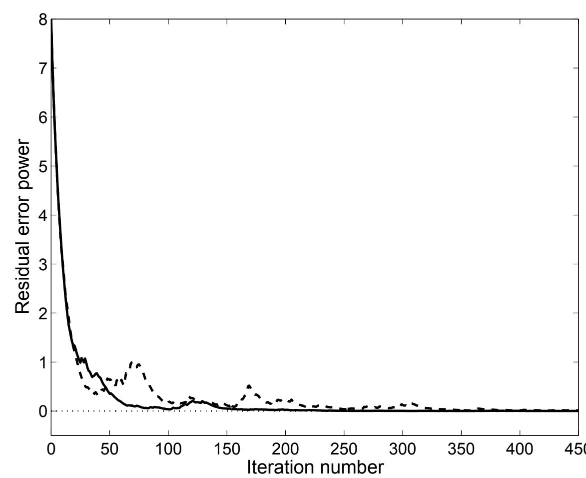

Fig. 5. *Evolution of residual error for different projection orders ($N = 3$ (dashed line) and $N = 7$ (solid line)), and $\mu = 0{,}02$ in lineal units compared with the theoretical MSE value (dotted line).*